Title	Photoisomerization reaction of CH2BrI following A-band and B-band photoexcitation in the solution phase: Transient resonance Raman observation of the iso-CH2I–Br photoproduct
Author(s)	Zheng, X; Phillips, DL
Citation	Journal of Chemical Physics, 2000, v. 113 n. 8, p. 3194-3203
Issued Date	2000
URL	http://hdl.handle.net/10722/42350
Rights	Creative Commons: Attribution 3.0 Hong Kong License

Photoisomerization reaction of CH_2BrI following *A*-band and *B*-band photoexcitation in the solution phase: Transient resonance Raman observation of the iso-CH_2I–Br photoproduct

Xuming Zheng and David Lee Phillips[a)]
Department of Chemistry, University of Hong Kong, Pokfulam Road, Hong Kong

(Received 9 May 2000; accepted 22 May 2000)

We present nanosecond transient resonance Raman experiments that investigate the photoproduct species formed following *A*-band and *B*-band excitation of bromoiodomethane in room temperature cyclohexane solutions. Density functional theory calculations were also performed for several species that have been proposed as photoproducts for photodissociation of bromoiodomethane in the condensed phase. Comparison of the experimental resonance Raman spectra to density functional theory computational results and results for the closely related iso-CH_2I–I and iso-CH_2Br–Br species demonstrated that the iso-CH_2I–Br species is mainly responsible for a transient absorption spectrum that appears after either *A*-band or *B*-band photoexcitation of bromoiodomethane in cyclohexane solution. This is in contrast to previous results for low temperature (12 K) solids where mainly the iso-CH_2Br–I species was observed following *A*-band photoexcitation of bromoiodomethane. Further density functional theory computational results indicate that the iso-CH_2I–Br species is noticeably more stable than the iso-CH_2Br–I species by about 4.1 kcal/mol. This suggests that although both iso-CH_2I–Br and iso-CH_2Br–I species may be initially produced following ultraviolet excitation of bromoiodomethane in cyclohexane solution, only the more stable isomer has a sufficiently long lifetime to be observed in our nanosecond time-scale transient resonance Raman experiments. We compare results for the bromoiodomethane ultraviolet photodissociation/photoisomerization reactions in the condensed phase to those of the closely related diiodomethane system and discuss a probable mechanism for the formation of the iso-bromoiodomethane species in the condensed phase. © *2000 American Institute of Physics.* [S0021-9606(00)00532-8]

I. INTRODUCTION

Dihalomethanes are of interest in atmospheric chemistry since they may be an important source of organoiodine and organobromine compounds emitted into the atmosphere.[1–6] A recent study attempted to assess the importance of diiodomethane, dibromomethane, and bromoiodomethane as possible sources for reactive halogens in the troposphere and in the marine boundary layer.[6] Dihalomethanes are also of interest for use in organic synthesis reactions such as cyclopropanation of alkenes.[7–14] For example, ultraviolet photoexcitation of diiodomethane in the solution phase has long been used for cyclopropanation of alkenes.[8–11] Bromoiodomethane has also been used as a prototype to examine bond selective electronic excitation and photochemistry.[15–19]

Molecular beam experiments have shown that photoexcitation within the *A*-band and *B*-band absorption transitions of bromoiodomethane leads to bond selective photodissociation.[15–17] Anisotropy measurements in these molecular beam experiments[15–17] determined that the bond selective photodissociation reactions occur much faster than molecular rotation (e.g., in a direct manner). Excitation with 210 nm light within the *B*-band absorption band of bromoiodomethane leads to a preference for cleavage of the C–Br bond with no cleavage of the C–I bond by itself.[16,17] Photoexcitation within the *A*-band absorption of bromoiodomethane leads predominantly to cleavage of the C–I bond[15–17] similar to iodoalkane *A*-band photodissociation reactions. The gas and solution phase absorption spectra of bromoiodomethane are very similar to one another.[18,19] Resonance Raman spectra and an intensity analysis investigation found that short-time photodissociation dynamics have multidimensional character with dynamics consistent with an impulsive ''semirigid'' radical model qualitative description of the photodissociation reactions (the C–I bond lengthens while the CH_2Br radical part moves toward a more planar structure upon *A*-band photoexcitation and the C–Br lengthens while the CH_2I radical part moves toward a more planar structure following *B*-band photoexcitation).[18,19] The resonance Raman spectra and associated short-time dynamics were consistent with the results of molecular beam experiments, which indicate a preference for C–Br bond cleavage following *B*-band photoexcitation and C–I bond cleavage subsequent to *A*-band photoexcitation of bromoiodomethane.

In this paper we report nanosecond transient resonance Raman experiments that examine the photoproducts produced following *A*-band and *B*-band photoexcitation of bromoiodomethane in cyclohexane solution. Density functional

a)Author to whom correspondence should be addressed; electronic mail: phillips@hkucc.hku.hk

theory computations were also done for several species that may be formed from the ultraviolet excitation of bromoiodomethane. Comparison of the experimental transient resonance Raman vibrational frequencies to the results of the density functional theory computations indicates that the iso-CH_2I–Br photoproduct is produced in noticeable amounts and is mainly responsible for the ~360–400 nm transient absorption band formed following ultraviolet photoexcitation of bromoiodomethane in the solution phase. However, ultraviolet excitation of bromoiodomethane in low temperature (12 K) solid state matrices led to the observation of the iso-CH_2Br–I species by Maier and co-workers using infrared absorption and ultraviolet/visible absorption spectroscopies.[20,21] Thus, room temperature solution phase ultraviolet (*A*-band or *B*-band) photoexcitation of bromoiodomethane leads to mostly iso-CH_2I–Br, while similar photoexcitation in low temperature (12 K) solid state matrices[20,21] gives mainly observation of the iso-CH_2Br–I species but not the iso-CH_2I–Br species. Additional density functional theory calculations were done to examine the relative stability of the iso-CH_2Br–I and iso-CH_2I–Br species. We compare the results for bromoiodomethane with previous results for diiodomethane and discuss possible mechanism(s) for the formation of the iso-CH_2Br–I and iso-CH_2I–Br species that may be consistent with the previous low temperature solid state results[20,21] and our present solution phase results.

II. EXPERIMENT

Bromoiodomethane was synthesized according to the method given by Miyano and Hashimoto[22] and its purity was determined by nuclear magnetic resonance and UV/visible spectroscopy (94%–98% for the samples used). Solutions with ~0.15 M concentration of bromoiodomethane in spectroscopic grade cyclohexane solvent (Aldrich Chemical Company) were used in the resonance Raman experiments. The experimental apparatus and methods have been detailed previously[23–27] so only a brief description will be given here. The excitation wavelengths for the two-color transient resonance Raman experiments were supplied by the harmonics and/or the hydrogen Raman shifted laser lines of the harmonics of a nanosecond pulsed Nd:YAG laser. Pump–probe delays of ~0 and 10 ns (set using an optical delay) were used to obtain the transient resonance Raman experiments. The pump and probe laser beams were loosely focused onto a flowing liquid stream of sample using near a collinear and backscattering geometry. The resonance Raman scattering was acquired using reflective optics and imaged through a depolarizer and entrance slit of a 0.5 m spectrograph equipped with a 1200 groove/mm grating blazed at 250 nm. The spectrograph grating dispersed the Raman scattered light onto a liquid nitrogen cooled charge-couple device (CCD) detector mounted on the exit port of the spectrograph. The Raman signal was collected by the CCD detector for 180–300 s before being readout to an interfaced PC computer and 10–30 of these readouts were added together to obtain the resonance Raman spectrum. Pump only, probe only, and pump–probe resonance Raman spectra were obtained. A background scan was also acquired. Subtraction of the probe only and pump only spectra from the pump–probe spectrum was done to subtract the solvent and parent compound Raman bands from the pump–probe resonance Raman spectrum and obtain the transient resonance Raman spectrum. The known vibrational frequencies of the cyclohexane solvent bands were used to calibrate the Raman shifts (in cm^{-1}) of the resonance Raman spectra.

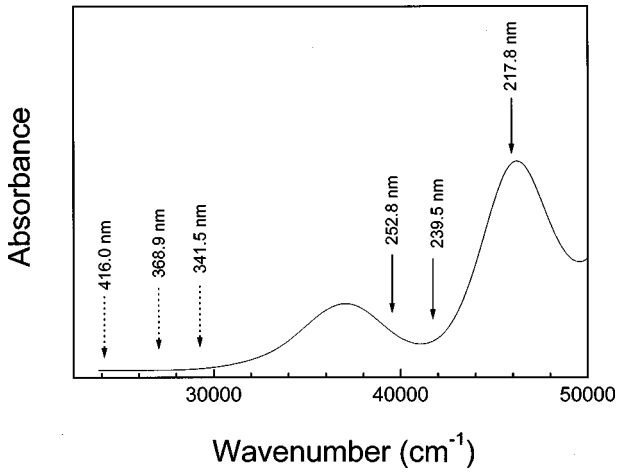

FIG. 1. Absorption spectrum of bromoiodomethane in cyclohexane solution with the pump (solid arrows) and probe (dashed arrows) excitation wavelengths (in nanometers) for the transient resonance Raman experiments shown above the spectrum.

III. CALCULATIONS

The Gaussian program suite (G98W) was used for all of the density functional theory computations presented here.[28] Complete geometry optimization and vibrational frequency computations were done analytically using C_1 symmetry using the B3LYP level of theory.[28,29] The electronic absorption transition energies were calculated using time-dependent density functional theory at random phase approximation [TD(RPA)][30] for the species investigated. Sadlej-PVTZ and aug-cc-PVTZ basis sets were used for all of the density functional theory calculations.[31,32]

IV. RESULTS AND DISCUSSION

A. Transient resonance Raman spectra and density functional theory calculations

Figure 1 shows the ultraviolet absorption spectrum of bromoiodomethane in cyclohexane solution and the excitation wavelengths used for the pump and probe beams of the transient resonance Raman experiments are indicated above the spectrum. The *A*-band and *B*-band absorption transitions are primarily due to $n \rightarrow \sigma^*$ transitions localized on the C–I C–Br chromophores respectively.[15–19] Photoexcitation of bromoiodomethane within the *A*-band absorption results in mainly C–I bond cleavage in the gas phase to give CH_2Br and iodine atom fragments, while *B*-band excitation leads mainly to C–Br bond cleavage (59% to CH_2I+Br channel) or cleavage of both C–Br and C–I bonds (~35% to CH_2+Br+I channel and ~6% to CH_2+IBr^*).[15–17] Figure 2 presents a typical probe only resonance Raman spectrum (A), a pump only spectrum in the probe wavelength region

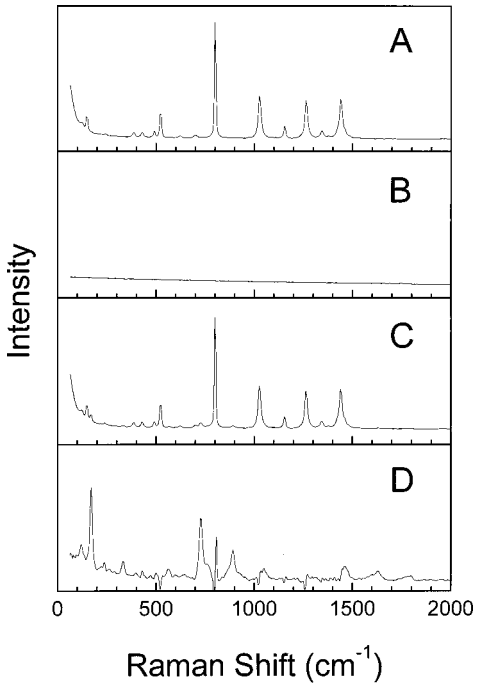

FIG. 2. Example of a typical probe only 341.5 nm Raman spectrum (A), pump only 239.5 nm spectrum in the probe wavelength region (B), a pump–probe (239.5 nm/341.5 nm) Raman spectrum (C), and the resulting transient resonance Raman spectrum (D) of the bromoiodomethane photoproduct.

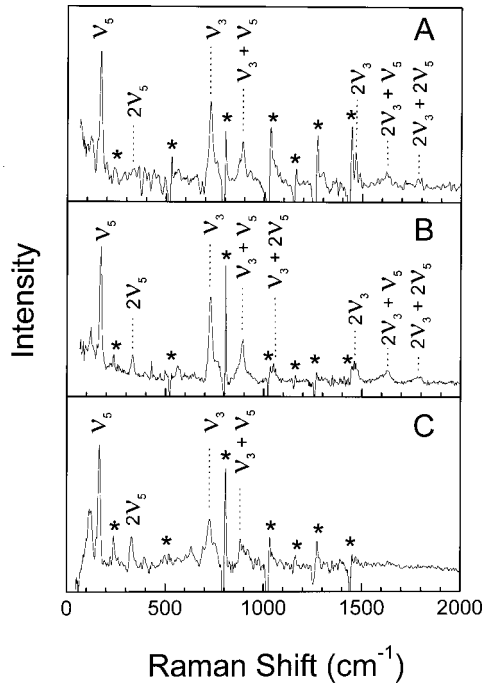

FIG. 3. Transient resonance Raman spectrum of the bromoiodomethane photoproduct (iso-CH_2I–Br) obtained for 252.7 nm pump/368.9 nm probe (top) 239.5 nm pump/341.5 nm probe (middle) and 217.8 nm pump/341.5 nm probe (bottom) excitation wavelengths. The asterisks mark regions where subtraction artifacts are present. The tentative assignments of the larger transient resonance Raman bands are shown above the spectra (see the text).

(B), a pump–probe resonance Raman spectrum (C), and the resulting transient resonance Raman spectrum of the photoproduct species (D) obtained after subtracting the pump only and probe only spectra from the pump–probe Raman spectrum. Figure 3 shows the transient resonance Raman spectra of the photoproduct species formed following ultraviolet photoexcitation with 252.7 nm (*A*-band), 239.5 nm (in between *A*-band and *B*-band), and 217.8 nm (*B*-band) pump wavelengths. The probe wavelengths for the transient Raman spectra shown in Fig. 3 are 368.9, 341.5, and 341.5 nm, respectively. Similar experiments were also done with 398.0 and 416.0 nm probe wavelengths but photoproduct spectra were not seen with these probe wavelengths following ultraviolet photoexcitation of bromoiodomethane in cyclohexane solution. The transient resonance Raman spectra of the photoproduct species displayed in Fig. 3 have most of their Raman intensity in the fundamentals, combination bands, and overtones of three Franck–Condon active modes whose fundamentals are at ~118, 173, and 730 cm^{-1}. In particular, the 173 and 730 cm^{-1} vibrational modes display noticeable intensity in their overtones and combination bands with each other. In order to help assign the transient resonance Raman spectra, we have done density functional theory computations for several species that have been proposed as being photoproducts of bromoiodomethane following photoexcitation within its *A*-band absorption and several other related compounds.

The parameters for the optimized geometries and vibrational frequencies obtained from the density functional theory calculations (B3LYP with either Sadlej-PVTZ or aug-cc-PVTZ basis sets) are shown in Tables I and II, respectively, for the iso-CH_2I–Br, iso-CH_2Br–I, CH_2BrI, CH_2BrI^+, CH_2Br, CH_2I, iso-CH_2I–I, and iso-CH_2–Br–Br species. Inspection of Table I shows that the iso-CH_2I–Br species has a C–I bond length very similar to that previously found for the iso-CH_2I–I species (1.960 and 1.957 Å, respectively) and iso-CH_2Br–I species has a C–Br bond length similar to that computed for iso-CH_2Br–Br (1.781 and 1.768 Å, respectively).[33,34] However, the I–Br bond lengths are significantly different from one another in the iso-CH_2I–Br and iso-CH_2Br–I species (2.790 and 2.926 Å, respectively).

These results suggest that the nominal C–I stretch, C–Br stretch, and I–Br stretch vibrational modes will be useful in distinguishing the iso-CH_2I–Br and iso-CH_2–Br–I species and that it may be useful to compare the iso-CH_2I–Br species to the iso-CH_2I–I species and the iso-CH_2Br–I species to the iso-CH_2Br–Br species. Table II presents the vibrational frequencies obtained from the density functional theory calculations for the iso-CH_2I–Br, iso-CH_2Br–I, CH_2BrI, CH_2BrI^+, CH_2Br, CH_2I, iso-CH_2I–I, and iso-CH_2–Br–Br species and compares them to experimental vibrational frequencies (from resonance Raman or infrared absorption spectra) where available. We note that the B3LYP/Sadlej-PVTZ computed vibrational frequencies agree very well with the Raman vibrational frequencies for the CH_2BrI molecule (especially for those vibrational modes below 1200 cm^{-1}). In addition there is also reasonable agreement for the iso-CH_2I–I and iso-CH_2Br–Br species between the B3LYP/Sadlej-PVTZ vibrational frequencies and the observed Raman and infrared experimental vibrational frequencies.[33,34] This suggests that corresponding B3LYP/

TABLE I. Parameters for the optimized geometry computed from the B3LYP density functional theory computations for iso-CH_2I–Br, iso-CH_2Br–I, CH_2BrI, CH_2BrI^+, CH_2Br, CH_2I, iso-CH_2I–I, and iso-CH_2Br–Br. Bond lengths are in angstroms and bond angles are in degrees.

Parameter	B3LYP computed value
Iso-CH_2I–Br	Using Sadlej-PVTZ basis set
C–I_1	1.960
I_1–Br_2	2.790
C–H_3, C–H_4	1.093
C–I_1–Br_2	121.0
I_1–C–H_3, I_1–C–H_4	118.4
H_3–C–H_4	119.7
D(H_3–C–I_1–Br_2), D(H_3–C–I_1–Br_2)	±79.6
Iso-CH_2Br–I	Using Sadlej-PVTZ basis set
C–Br_1	1.781
Br_1–I_2	2.926
C–H_3, C–H_4	1.092
C–Br_1–I_2	123.2
Br_1–C–H_3, Br_1–C–H_4	117.6
H_3–C–H_4	121.6
D(H_3–C–Br_1–I_2), D(H_3–C–Br_1–I_2)	±79.9
CH_2BrI	Using Sadlej-PVTZ basis set
C–Br	1.946
C–I	2.155
C–H_3, C–H_4	1.094
Br–C–I	115.3
Br–C–H_3, Br–C–H_4	107.4
I–C–H_3, I–C–H_4	107.5
H_3–C–H_4	111.8
Br–ClH_3	−119.8
H_3–CH_4Br	−117.6
CH_2BrI^+	Using Sadlej-PVTZ basis set
C–Br	1.899
C–I	2.146
C–H_3, C–H_4	1.107
Br–C–I	112.0
Br–C–H_3, Br–C–H_4	109.3
I–C–H_3, I–C–H_4	104.7
H_3–C–H_4	108.3
Br–ClH_3	−124.1
H_3–CH_4Br	−119.0
CH_2Br[a]	Using aug-cc-PVTZ basis set
C–Br	1.858
C–H_1, C–H_2	1.075
Br–C–H_1, Br–C–H_2	117.7
H_1–C–H_2	124.6
H_1–CH_2Br	180.0
CH_2I[b]	Using Sadlej-PVTZ basis set
C–I	1.858
C–H_1, C–H_2	1.075
I–C–H_1, I–C–H_2	117.7
H_1–C–H_2	124.6
H_1–CH_2I	180.0
Iso-CH_2I–I[b]	Using Sadlej-PVTZ basis set
C–I_1	1.957
I_1–I_2	3.042
C–H_3, C–H_4	1.091
C–I_1–I_2	118.2
I_1–C–H_3, I_1–C–H_4	119.1
D(H_3–C–I_1–I_2), D(H_4–C–I_1–I_2)	90.0
Iso-CH_2Br–Br[a]	Using aug-cc-PVTZ basis set
C–Br_1	1.768
Br_1–Br_2	2.674
C–H_3, C–H_4	1.078
C–Br_1–Br_2	122.0
Br_1–C–H_3, Br_1–C–H_4	118.1
H_3–C–H_4	121.6
D(H_3–C–Br_1–Br_2), D(H_3–C–Br_1–Br_2)	±80.7

[a]From Ref. 34.
[b]From Ref. 33.

Sadlej-PVTZ computations will be useful in predicting the vibrational frequencies of the iso-CH_2I–Br and iso-CH_2Br–I species. Since there are clearly three low frequency fundamental vibrational modes in the Raman spectrum of Fig. 3 (top) (e.g., the ~118, 173, and 730 cm^{-1} Raman bands), we can rule out the CH_2Br and CH_2I radicals as the photoproduct species being responsible for the transient resonance Raman spectrum of Fig. 3 because these radicals have only one low frequency A_1 vibrational mode (703 cm^{-1} for CH_2Br and 614 cm^{-1} for CH_2I). Similarly, the CH_2BrI molecule and the CH_2BrI^+ radical cation cannot be assigned to the photoproduct Raman spectrum of Fig. 3 since they have only one A_1 vibrational mode below 200 cm^{-1} (143 cm^{-1} for CH_2BrI and 153 cm^{-1} for the CH_2BrI^+ radical cation) while the photoproduct Raman spectrum of Fig. 3 has two fundamental bands below 200 cm^{-1} (~118 and 173 cm^{-1}). The presence of two low frequency A_1 fundamental bands below 200 cm^{-1} appears to be characteristic of iso-dihalomethane species. For example, iso-CH_2I–I exhibits two A_1 vibrational modes below 200 cm^{-1} (computed to be at 128 and 99 cm^{-1})[33] as does iso-CH_2Br–Br (computed to be at 180 and 133 cm^{-1}).[34] This is also the case for the iso-CH_2I–Br (computed to be at 165 and 106 cm^{-1}) and iso-CH_2Br–I (computed to be at 148 and 120 cm^{-1}) species shown in Table II. Therefore we tentatively assign the transient resonance Raman spectrum of the photoproduct obtained for *A*-band photoexcitation of bromoiodomethane in cyclohexane solution shown in Fig. 3 to an iso-bromoiodomethane species. To pin down this assignment further it is instructive to compare the iso-CH_2I–Br species to iso-CH_2I–I and the iso-CH_2Br–I species to iso-CH_2Br–Br. Figure 4 compares the transient resonance Raman spectra for iso-CH_2I–I (middle) and iso-CH_2Br–Br (bottom) to that found for the iso-bromoiodomethane species (top) obtained following ultraviolet excitation of bromoiodomethane in cyclohexane solution.

The B3LYP/Sadlej-PVTZ computed nominal C–I stretch vibrational mode is at 782 cm^{-1} for iso-CH_2I–Br and 755 cm^{-1} for iso-CH_2I–I, which compares reasonably well with the experimental resonance Raman frequencies of 730 cm^{-1} for the photoproduct spectrum found following *A*-band photoexcitation of bromoiodomethane in Fig. 3 and the 701 cm^{-1} Raman band found previously for iso-CH_2I–I, respectively.[33] It is interesting that the difference between the computed value and the resonance Raman experiment value are almost the same for the ν_3 nominal C–I stretch vibration in iso-CH_2I–Br (a 52 cm^{-1} difference) and iso-CH_2I–I (a 54 cm^{-1} difference).[33] The computed value for the C–Br stretch vibration is 840 cm^{-1} for the iso-CH_2Br–I species, and this is substantially higher than the 730 cm^{-1} experimental Raman band observed for the photoproduct produced after ultraviolet excitation of bromoiodomethane in the solution phase. It is very useful to compare the halogen–halogen stretch vibrational modes among the different iso-dihalomethane species. We note that the B3LYP computations predict this vibrational frequency very well with excellent agreement found with the vibrational frequencies obtained from resonance Raman experiments for iso-CH_2I–I and iso-CH_2Br–Br (see Table II).[33,34]

TABLE II. Comparison of experimental vibrational frequencies (in cm^{-1}) found from transient resonance Raman spectra and previously reported infrared absorption experiments (Refs. 20 and 21) to the B3LYP calculated vibrational frequencies. The corresponding vibrational frequencies for the fully deuterated compounds are given in parentheses.

Vibrational mode	B3LYP calc	Resonance Raman	Infrared absorption
Iso-CH_2I–Br (iso-CD_2I–Br)	Sadlej-PVTZ basis set	This work	
A' ν_1, CH_2 sym. str.	3115 (2251)		
ν_2, CH_2 def.	1357 (1024)		
ν_3, C–I str.	782 (646)	730	
ν_4, CH_2 wag	671 (541)		
ν_5, I–Br str.	165 (164)	173	
ν_6, C–I–Br bend	106 (99)	118	
A'' ν_7, CH_2 asym. str.	3257 (2430)		
ν_8, CH_2 rock	867 (693)		
ν_9, CH_2 twist	469 (337)		
Iso-CH_2Br–I (iso-CD_2Br–I)	Sadlej-PVTZ basis set		From Refs. 20 and 21
A' ν_1, CH_2 sym. str.	3115 (2248)		~3036 (~2222)
ν_2, CH_2 def.	1377 (1042)		··· (~1055)
ν_3, C–Br str.	840 (707)		··· (~708)
ν_4, CH_2 wag	698 (560)		~631 (~505)
ν_5, I–Br str.	148 (147)		
ν_6, C–I Br bend	120 (112)		
A'' ν_7, CH_2 asym. str.	3271 (2445)		~3165 (~2390)
ν_8, CH_2 rock	945 (755)		
ν_9, CH_2 twist	429 (309)		
CH_2BrI (CD_2BrI)	Sadlej-PVTZ basis set	From Ref. 19	
A' ν_1, CH_2 sym. str.	3108 (2252)	2978	
ν_2, CH_2 def.	1393 (1021)	1374	
ν_3, CH_2 wag.	1154 (867)	1150	
ν_4, C–Br str.	612 (584)	616	
ν_5, C–I str.	522 (494)	517	
ν_6, I–C Br bend	143 (142)	144	
A'' ν_7, CH_2 asym. str.	3203 (2385)	3053	
ν_8, CH_2 twist	1077 (764)	1065	
ν_9, CH_2 rock	746 (582)	754	
CH_2BrI^+ (CD_2BrI^+)	Sadlej-PVTZ basis set		
A' ν_1, CH_2 sym. str.	2995 (2172)		
ν_2, CH_2 def.	1283 (937)		
ν_3, CH_2 wag.	1056 (781)		
ν_4 C–Br str.	659 (629)		
ν_5, C–I str.	464 (448)		
ν_6, I–C Br bend	153 (152)		
A'' ν_7, CH_2 asym. str.	3027 (2235)		
ν_8, CH_2 twist	994 (708)		
ν_9, CH_2 rock	433 (342)		
Iso-CH_2I–I (iso-CD_2I–I)	Sadlej-PVTZ basis set	From Ref. 33	From Refs. 20 and 21
A' ν_1, CH_2 sym. Str.	3131 (2260)	···	3028 (2213)
ν_2, CH_2 scissor	1340 (1011)	···	1373 (1041–1033)
ν_3 C–I str.	**755 (645)**	**701 (640)**	**714/705 (645)**
ν_4, CH_2 wag	619 (476)	619 (496)	622-611 (498-486)
ν_5, I–I str.	**128 (128)**	**128 (128)**	···
ν_6, C–I–I bend	99 (93)	? (~110)	···
A'' ν_7, CH_2 asym. str.	3281 (2451)	···	3151 (2378)
ν_8, CH_2 rock	865 (697)	···	···
ν_9, CH_2 twist	447 (318)	487 ? (352 ?)	···
Iso-CH_2Br–Br (iso-CD_2Br–Br)	aug-cc-PVTZ basis set	From Ref. 34	From Refs. 20 and 21
A' ν_1, CH_2 sym. Str.	3152 (2275)	···	3030 (2213)
ν_2, CH_2 scissor	1428 (1078)	···	1334 (1030)
ν_3, C–Br str.	858 (771)	···	··· (732)
ν_4, CH_2 wag	738 (594)	690	684,695
ν_5, Br–Br str.	**180 (180)**	**176**	···
ν_6, C–Br–Br bend	133 (124)	146	···
A'' ν_7, CH_2 asym. str.	3286 (2456)	···	3156 (2384)
ν_8, CH_2 rock	966 (724)	960	···
ν_9, CH_2 twist	468 (337)	480 ?	···

TABLE II. (*Continued*.)

Vibrational mode	B3LYP calc	Resonance Raman	Infrared absorption
CH_2Br (CD_2Br)	aug-cc-PVTZ basis set		
A_1 ν_1, CH sym Str.	3172 (2284)		
ν_2, CH_2 def.	1382 (1029)		
ν_3, C–Br str.	703 (662)		
B_1 ν_4, CH_2 wag	152 (118)		
B_2 ν_5, CH asym. Str.	3325 (2488)		
ν_6, CH_2 rock	926 (691)		
CH_2I (CD_2I)	Sadlej-PVTZ basis set		
A_1 ν_1, CH sym. Str.	3126 (2252)		
ν_2, CH_2 def.	1309 (974)		
ν_3 C–I str.	614 (576)		
B_1 ν_4, CH_2 wag	234 (180)		
B_2 ν_5, CH asym. Str.	3288 (2457)		
ν_6, CH_2 rock	832 (619)		

For example, the computed vibrational frequency for the nominal I–I stretch (ν_5) in iso-CH_2–I–I is 128 cm^{-1}, which is the same as that observed in the resonance Raman experiments (128 cm^{-1}), and the Br–Br stretch (ν_5) was calculated to be 180 cm^{-1}, which is very close to the 176 cm^{-1} observed in the resonance Raman spectra for iso-CH_2Br–Br. It would appear reasonable that a similar level of agreement might be found for the I–Br stretch in the iso-CH_2I–Br and iso-CH_2Br–I species. The I–Br bond is significantly different for the optimized geometry of the iso-CH_2I–Br (2.790 Å) and iso-CH_2Br–I (2.926 Å) species shown in Table I. The corresponding I–Br vibrational frequencies (ν_5) shown in Table II are also significantly different for the iso-CH_2I–Br (computed value of 165 cm^{-1}) and iso-CH_2Br–I (computed value of 148 cm^{-1}) species. This indicates the I–Br stretch vibrational mode is diagnostic of which iso-bromoiodomethane species is present. The nanosecond transient resonance Raman spectrum found for the photoproduct formed following ultraviolet photoexcitation of bromoiodomethane in cyclohexane solution has a strong Raman fundamental band at 173 cm^{-1} that can be easily assigned to the I–Br stretch vibrational mode of the iso-CH_2I–Br species (computed to be at 165 cm^{-1}) but not the iso-CH_2Br–I species (computed to be at 148 cm^{-1}). The agreement between the calculated and experimental values of the I–Br stretch vibrational mode for iso-CH_2I–Br is very similar to that previously found for the I–I vibration in iso-CH_2I–I and the Br–Br vibration in iso-CH_2Br–Br.[33,34] The experimental resonance Raman band at ~118 cm^{-1} can then be assigned to the nominal C–I–Br bend (computed value at 106 cm^{-1}). We note that the agreement between the computed and experimental values for the C–I–Br bend mode in iso-CH_2I–Br (a difference of 12 cm^{-1}) is similar to that found for the C–I–I bend mode in iso-CH_2I–I (a difference of 17 cm^{-1} for iso-CD_2I–I).[33] Comparison of the resonance Raman spectrum for iso-CH_2I–I (Fig. 4 (middle) with the photoproduct resonance Raman spectrum we ascribe to the iso-CH_2I–Br species [see Figs. 3 and 4 (top)]) shows that they have very similar intensity patterns. The intensity in the halogen–I stretch (ν_5) and C–I stretch (ν_3) Franck–Condon active modes is intense for both iso-CH_2I–I and iso-CH_2I–Br, with both modes displaying noticeable intensity in their overtones and combination bands with each other. In summary, comparison of the B3LYP computational results and experimental results for the closely related iso-CH_2I–I and iso-CH_2Br–Br species to those for the iso-bromoiodomethane species indicates that the transient resonance Raman spectrum of the photoproduct formed following ultraviolet excitation of bromoiodomethane in cyclohexane solution should be assigned to the iso-CH_2I–Br species.

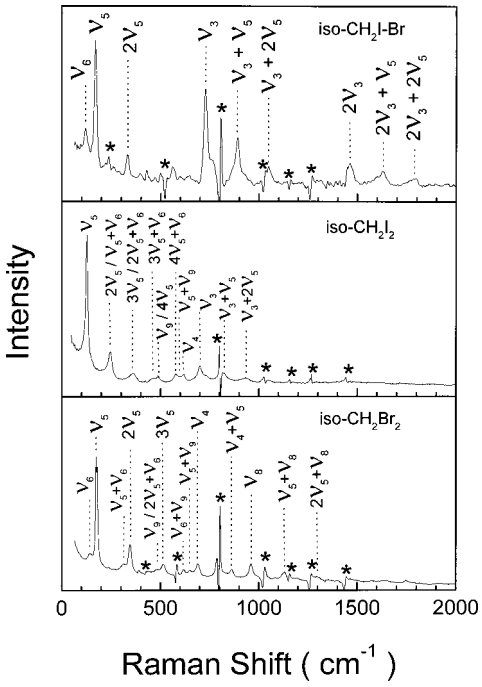

FIG. 4. Transient resonance Raman spectrum of the bromoiodomethane photoproduct (iso-CH_2I–Br) obtained for 239.5 nm pump/341.5 nm probe excitation wavelengths is shown at the top. Transient resonance Raman spectra for iso-CH_2I–I (309.1 nm pump and 416.0 nm probe excitation wavelengths) and iso-CH_2Br–Br (266.0 pump and 341.5 nm probe excitation wavelengths) are shown for comparison purposes at the middle and bottom, respectively.

TABLE III. Electronic absorption transition energies obtained from density functional theory calculations for iso-CH_2I–Br, iso-CH_2Br–I, CH_2BrI^+, CH_2Br, and CH_2I. The calculated oscillator strengths are given in parentheses.

Molecule	URPA//UB3LYP/Sadlej-PVTZ
Iso-CH_2I–Br	Singlet transitions
	373.14 nm (0.0005)
	358.45 nm (0.4582)
	320.19 nm (0.0166)
	318.91 nm (0.0000)
	302.22 nm (0.0000)
	280.54 nm (0.0000)
	260.51 nm (0.0002)
	250.04 nm (0.0240)
	210.52 nm (0.0770)
Iso-CH_2Br–I	
	493.72 nm (0.0000)
	473.45 nm (0.0308)
	422.43 nm (0.5317)
	304.59 nm (0.0000)
	302.00 nm (0.0000)
	264.94 nm (0.0000)
	262.18 nm (0.0006)
	238.95 nm (0.0009)
	213.48 nm (0.1242)
CH_2BrI^+	486 nm (0.0017)
	314 nm (0.0021)
	276 nm (0.0003)
	254 nm (0.0000)
	246 nm (0.0001)
CH_2Br	Using aug-cc-PVTZ basis set (from Ref. 34)
	255 nm (0.0011)
	198 nm (0.0001)
	194 nm (0.0000)
CH_2I	(From Ref. 33)
	316 nm (0.0001)
	262 nm (0.0001)
	216 nm (0.0009)

We have previously used B3LYP time-dependent random phase computations (TD/RPA) to calculate electronic transition energies and oscillator strengths for CH_2I_2 and obtained reasonable agreement with the experimental spectra (within about 0.15–0.30 eV).[35] We have also performed similar calculations for the electronic transitions of the iso-CH_2I–Br, iso-CH_2Br–I, CH_2BrI^+, CH_2Br, and CH_2I species and the results for the singlet transitions are shown in Table III. The iso-CH_2I–Br species has a very intense electronic transition computed to be at 358 nm with an oscillator strength of 0.4582. This transition corresponds well with our assignment of the iso-CH_2I–Br species to the photoproduct transient resonance Raman spectrum formed from ultraviolet excitation of bromoiodomethane in cyclohexane solution. We performed similar transient resonance Raman experiments with 397.9 and 416.0 nm probe wavelengths and could detect no transient species which would be expected to correspond to the iso-CH_2Br–I species which has an intense calculated transition at ~422 nm with an oscillator strength of 0.5317 and an intense experimental absorption band ~403 nm in low temperature (12 K) solid matrices.[20,21] We also note that experiments done with similar probe wavelengths and conditions could readily detect the iso-CH_2I–I species (for probe wavelengths of 397.9 and 416.0 nm) and iso-CH_2Br–Br species (for 341.5 nm probe wavelength).[33,34] This also indirectly supports our assignment of the transient resonance Raman spectrum to the iso-CH_2I–Br species and not the iso-CH_2Br–I species.

Comparison of the infrared vibrational frequencies observed by Maier and co-workers[20,21] for iso-CH_2Br–I in low temperature matrices to results for both density functional theory computations and experimental spectra for iso-CH_2I–I and iso-CH_2Br–Br shown in Table II indicates that their assignment of the photoproduct species to iso-CH_2Br–I following ultraviolet excitation of bromoiodomethane is likely correct. For example, the C–I stretch and CH_2 wag fundamentals are both clearly seen in both the resonance Raman and infrared spectra of iso-CH_2I–I, while only the CH_2 wag fundamental is clearly seen in the iso-CH_2Br–Br infrared and Raman spectra and the C–Br stretch fundamental only shows up weakly in the iso-CH_2Br–Br infrared spectrum. The behavior of the observed infrared vibrational bands attributed to the iso-CH_2Br–I species is most similar to that of iso-CH_2Br–Br. Since the C–Br bond length is almost the same for the iso-CH_2Br–I and iso-CH_2Br–Br species it is most consistent to assign the infrared spectrum observed by Maier and co-workers[20,21] following excitation of bromoiodomethane in a low temperature solid to the iso-CH_2Br–I species as they did. This assignment is also consistent with the density functional theory computational results presented here.

B. Discussion of possible photochemical mechanism(s) for the formation of iso-CH_2I–Br from ultraviolet excitation of CH_2BrI in the solution phase

It appears that iso-CH_2I–Br is noticeably produced following ultraviolet photoexcitation in room temperature cyclohexane solution (this work), but iso-CH_2Br–I is observed after ultraviolet excitation of bromoiodomethane in low temperature solid state matrices.[20,21] How does the ultraviolet excitation of bromoiodomethane in the solution phase lead to the production of the iso-CH_2I–Br photoproduct we see in our transient resonance Raman spectra? To help answer this question, it is useful to examine the more extensively studied and closely related diiodomethane molecule. Ultraviolet excitation of diiodomethane in the gas phase results in direct C–I bond breakage to give CH_2I and I or I* photofragments.[36–39] Solution phase femtosecond transient absorption experiments for diiodomethane[40–42] also show that the initial process is C–I bond cleavage, similar to the results found for gas phase ultraviolet excitation of diiodomethane. The initial direct C–I bond cleavage of diiodomethane in the gas and solution phases is consistent with *A*-band resonance Raman investigations of the Franck–Condon region dynamics.[43–48] The three femtosecond transient absorption studies[40–42] display similar behavior with a fast rise segment of a few hundred femtoseconds due to the

initial C–I bond cleavage followed by a fast decay segment (usually ascribed to some geminate recombination) and then a slower rise component on the picosecond time scale. The interpretations offered for these femtosecond experiments varied a bit depending on their assignment of the species responsible for the transient absorption.[40–42] We recently reported a nanosecond transient resonance Raman investigation to elucidate the species responsible for the characteristic ~385 nm transient absorption band observed following ultraviolet excitation of diiodomethane in the condensed phase.[33] Comparison of our transient resonance Raman spectra to density functional theory computational results for several proposed photoproduct species and previous infrared spectra obtained for dihalomethane isomers in low temperature solids clearly demonstrated that the iso-CH_2I–I species is responsible for the ~385 nm transient absorption band (at least on the nanosecond time scale). Inasmuch as the transient absorption band ~385 nm seen on the ultrafast time scale is the same as the one observed on the nanosecond time scale, the basic mechanism proposed by Åkesson and co-workers[42] is probably correct. They indicated that ultraviolet excitation of diiodomethane in room temperature solutions leads to a fast C–I bond scission to give CH_2I and I fragments which then collide with the solvent cage to give some recombination to form a hot iso-CH_2I–I photoproduct that then cools to give a thermalized iso-CH_2I–I photoproduct than can be observed at later times.[42] Therefore, recombination of the CH_2I and I photofragments within the solvent cage appears to form enough iso-CH_2I–I photoproduct so it can be observed in room temperature solutions. It is very likely that a similar mechanism would result in the noticeable formation of iso-bromoiodomethane following ultraviolet excitation in room temperature solutions.

The situation for bromoiodomethane is somewhat more complicated, since it has two different carbon–halogen chromophores (C–I and C–Br) that are responsible for its ultraviolet absorption spectrum. Molecular beam experiments indicate that some amount of C–I and C–Br bond cleavage occurs in both the *A*-band and *B*-band absorption transitions, with more C–I bond cleavage taking place in the *A* band and more C–Br bond breakage taking place in the *B* band.[15–17] For example, Bersohn and co-workers[15] found that broadband excitation of bromoiodomethane in the *A*-band absorption (mainly the 260–320 nm region using a Hg–Xe lamp with a filter solution) results in about 86% C–I bond cleavage to give CH_2Br and I fragments and 14% C–Br bond cleavage to give CH_2I and Br fragments. Further work done by Butler and Lee and co-workers[16,17] showed that 248.5 nm excitation within the *A* band results in both C–I bond cleavage (to give CH_2Br and I fragments) and C–Br bond cleavage (to give CH_2I and Br fragments), with the C–I bond cleavage channel being the predominant channel by at least 1.2 to 1.0. *B*-band (210 nm) excitation of bromoiodomethane resulted in about 59% C–Br bond cleavage (to give CH_2I and I fragments), ~33%–35% simultaneous C–Br and C–I bond cleavage (to give CH_2+I+Br fragments), and about 6% simultaneous C–Br and C–I bond cleavage (to give CH_2 and electronically excited IBr fragments).[17] Assuming the mechanism found for ultraviolet excitation of diiodomethane in room temperature solutions is applicable to the direct photodissociation reactions of bromoiodomethane, we may reasonably expect some initial formation of both the iso-CH_2I–Br and iso-CH_2Br–I species following both *A*-band and *B*-band excitation of bromoiodomethane. Since the C–I bond breaking is preferred for *A*-band excitation and C–Br bond breaking is more preferred for *B*-band excitation, one could expect that formation of the iso-CH_2Br–I species would be preferred following *A*-band excitation and the iso-CH_2I–Br species would be preferred following *B*-band excitation. However, we only observe the iso-CH_2I–Br species following ultraviolet excitation of bromoiodomethane in room temperature cyclohexane solution on the nanosecond time scale. For low temperature solids (12 K), ultraviolet excitation of bromoiodomethane (mainly in the *A* band from 255 to 290 nm) leads to mostly formation of the iso-CH_2Br–I species.[20,21]

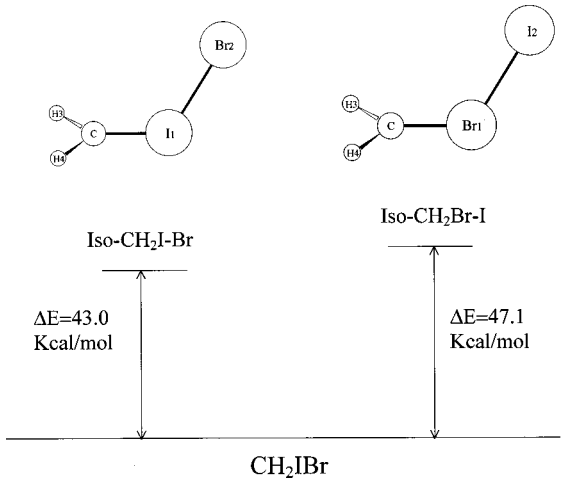

FIG. 5. Simple schematic diagram of the relative energies for the optimized equilibrium geometries of iso-CH_2I–Br, iso-CH_2Br–I, and CH_2BrI. The optimized geometry for iso-CH_2I–Br and iso-CH_2Br–I obtained from the density functional theory calculations (B3LYP/Sadlej-PVTZ) are shown at the top part.

In order to help learn more about this difference in reaction outcome with the condensed phase environment, we have done some additional density functional theory computations to explore the relative stability of the iso-CH_2I–Br and iso-CH_2Br–I isomers and the bromoiodomethane parent molecule. Our B3LYP/Sadlej-PVTZ computations indicate that the energy for the iso-CH_2I–Br molecule is about 43.0 kcal/mol above that for the parent bromoiodomethane molecule and the energy for the iso-CH_2Br–I molecule is about 47.1 kcal/mol above that for the parent bromoiodomethane molecule (see Fig. 5). The iso-CH_2I–Br isomer is noticeably more stable than the iso-CH_2Br–I isomer (by about 4.1 kcal/mol). A straightforward explanation for why our room temperature solution phase experiments on the nanosecond time scale only observe the iso-CH_2I–Br species and not the iso-CH_2Br–I species is that their different relative stability results in significantly different lifetimes in solution. For example, the iso-CH_2I–Br species probably has a substantially longer lifetime (and is observable on the nanosecond time

scale) while the iso-CH_2Br–I has a much shorter lifetime (and is not observed noticeably on the nanosecond time scale). This is consistent with the observed relative stability of iso-dihalomethanes found by Maier and co-workers from warming low temperature photoiosmers held in a polyethylene film.[21] They found that iso-CH_2I–I started to disappear above 100 K while iso-CH_2Br–I and iso-CH_2Cl–I had much lower stability and began to disappear at much lower temperatures ~26–30 K for iso-CH_2Cl–I, for example).[21] The iso-CH_2Br–I species predominantly observed in the low temperature (12 K) solid state experiments following broadband ultraviolet excitation of bromoiodomethane (mainly of the *A*-band)[20,21] appears reasonably consistent with the broadband excitation of the *A* band of bromoiodomethane molecular beam results of Bersohn and co-workers,[15] which show mostly C–I bond cleavage (86%) compared to C–Br bond cleavage (~14%). However, it is intriguing that no discernible perturbation of the infrared absorption spectra or transient absorption spectrum for the iso-CH_2Br–I photoproduct by the expected minor iso-CH_2I–Br photoproduct was reported. The colder and more rigid low temperature sold state matrices appear to efficiently trap the initially formed iso-bromoiodomethane species, while only the more stable isomer is observed in room temperature cyclohexane solutions on the nanosecond time scale. Our current results indicate that the iso-CH_2I–Br species is substantially more stable than the iso-CH_2Br–I species and this is also consistent with our present density functional theory results. The solvent caging also appears substantially different for the low temperature solids compared to room temperature liquids.

It would be very interesting to examine the wavelength-dependent behavior (*A* band versus *B* band) of the ultraviolet photodissociation reaction of bromoiodomethane in both room temperature liquids and low temperature solids. We note that details of the mechanism of formation of iso-bromoiodomethane photoproducts could be directly probed using ultrafast time-resolved experiments (such as transient absorption and/or vibrational spectroscopies) such as has been done for the closely related diiodomethane system.[40–42] These types of investigations would be interesting to elucidate how much bond selective photochemistry (e.g., relative formation of iso-CH_2Br–I and iso-CH_2I–Br species as a function of wavelength) survives as a function of time scale and molecular environment. Such studies would also be good for probing the details of solvent–solute interactions and solvent-induced caging effects on photodissociation/photoisomerization reactions in condensed phase environments.

ACKNOWLEDGMENTS

This work was supported by grants from the Research Grants Council (RGC) of Hong Kong, the Hung Hing Ying Physical Sciences Research Fund, the Committee on Research and Conference Grants (CRCG) from the University of Hong Kong, and the Large Items of Equipment Allocation 1993–94 from the University of Hong Kong.

[1] Th. Class and K. Ballschmiter, J. Atmos. Chem. **6**, 35 (1988).
[2] S. Klick and K. Abrahamsson, J. Geophys. Res. B **97**, 12 683 (1992).
[3] K. G. Heumann, Anal. Chim. Acta **283**, 230 (1993).
[4] R. M. Moore, M. Webb, R. Tokarczyk, and R. Wever, J. Petrol. **101**, 20 899 (1996).
[5] L. Carpenter, East Atlantic Spring Experiment (EASE) 1997 campaign.
[6] J. C. Mössigner, D. E. Shallcross, and R. A. Cox, J. Chem. Soc., Faraday Trans. **94**, 1391 (1998).
[7] H. E. Simmons and R. D. Smith, J. Am. Chem. Soc. **81**, 4256 (1959).
[8] D. C. Blomstrom, K. Herbig, and H. E. Simmons, J. Org. Chem. **30**, 959 (1965).
[9] N. J. Pienta and P. J. Kropp, J. Am. Chem. Soc. **100**, 655 (1978).
[10] P. J. Kropp, N. J. Pienta, J. A. Sawyer, and R. P. Polniaszek, Tetrahedron **37**, 3229 (1981).
[11] P. J. Kropp, Acc. Chem. Res. **17**, 131 (1984).
[12] E. C. Friedrich, J. M. Domek, and R. Y. Pong, J. Org. Chem. **50**, 4640 (1985).
[13] E. C. Freidrich, S. E. Lunetta, and E. J. Lewis, J. Org. Chem. **54**, 2388 (1989).
[14] S. Durandetti, S. Sibille, and J. Pérchon, J. Org. Chem. **56**, 3255 (1991).
[15] S. J. Lee and R. Bersohn, J. Phys. Chem. **86**, 728 (1982).
[16] L. J. Butler, E. J. Hintsa, and Y. T. Lee, J. Chem. Phys. **84**, 4104 (1986).
[17] L. J. Butler, E. J. Hintsa, and Y. T. Lee, J. Chem. Phys. **86**, 2051 (1987).
[18] S. Q. Man, W. M. Kwok, and D. L. Phillips, J. Phys. Chem. **99**, 15705 (1995).
[19] S.-Q. Man, W. M. Kwok, A. E. Johnson, and D. L. Phillips, J. Chem. Phys. **105**, 5842 (1996).
[20] G. Maier and H. P. Reisenauer, Angew. Chem. Int. Ed. Engl. **25**, 819 (1986).
[21] G. Maier, H. P. Reisenauer, J. Lu, L. J. Scaad, and B. A. Hess Jr., J. Am. Chem. Soc. **112**, 5117 (1990).
[22] S. Miyano and H. Hashimoto, Bull. Chem. Soc. Jpn. **44**, 2864 (1971).
[23] L. C. T. Shoute, D. Pan, and D. L. Phillips, Chem. Phys. Lett. **290**, 24 (1998).
[24] D. Pan, L. C. T. Shoute, and D. L. Phillips, Chem. Phys. Lett. **303**, 629 (1999).
[25] D. Pan and D. L. Phillips, J. Phys. Chem. A **103**, 4737 (1999).
[26] D. Pan, L. C. T. Shoute, and D. L. Phillips, J. Phys. Chem. A **103**, 6851 (1999).
[27] D. Pan, L. C. T. Shoute, and D. L. Phillips, Chem. Phys. Lett. **316**, 395 (2000).
[28] GAUSSIAN 98, Revision A.7, M. J. Frisch, G. W. Trucks, H. B. Schlegel, G. E. Scuseria, M. A. Robb, J. R. Cheeseman, V. G. Zakrzewski, J. A. Montgomery, Jr., R. E. Stratmann, J. C. Burant, S. Dapprich, J. M. Millam, A. D. Daniels, K. N. Kudin, M. C. Strain, O. Farkas, J. Tomasi, V. Barone, M. Cossi, R. Cammi, B. Mennucci, C. Pomelli, C. Adamo, S. Clifford, J. Ochterski, G. A. Petersson, P. Y. Ayala, Q. Cui, K. Morokuma, D. K. Malick, A. D. Rabuck, K. Raghavachari, J. B. Foresman, J. Cioslowski, J. V. Ortiz, A. G. Baboul, B. B. Stefanov, G. Liu, A. Liashenko, P. Piskorz, I. Komaromi, R. Gomperts, R. L. Martin, D. J. Fox, T. Keith, M. A. Al-Laham, C. Y. Peng, A. Nanayakkara, C. Gonzalez, M. Challacombe, P. M. W. Gill, B. Johnson, W. Chen, M. W. Wong, J. L. Andres, C. Gonzalez, M. Head-Gordon, E. S. Replogle, and J. A. Pople, Gaussian, Inc., Pittsburgh, PA, 1998.
[29] A. D. Becke, J. Chem. Phys. **98**, 1372 (1993).
[30] R. Bauernschmitt and R. Ahlrichs, Chem. Phys. Lett. **256**, 454 (1996).
[31] N. Godbout, D. R. Salahub, J. Andzelm, and E. Wimmer, Can. J. Chem. **70**, 560 (1992). Basis sets were obtained from the Extensible Computational Chemistry Environment Basis Set Database, Environmental and Molecular Sciences Laboratory, which is part of the Pacific Northwest Laboratory, P.O. Box 999, Richland, Washington 99352, and funded by the U.S. Department of Energy. The Pacific Northwest Laboratory is a multiprogram laboratory operated by Battele Memorial Institute for the U.S. Department of Energy under Contract No. DE-AC06-76RLO 1830. Contact David Feller or Karen Schuchardt for more information.
[32] A. J. Sadlej, Theor. Chim. Acta **81**, 339 (1992).
[33] X. Zheng and D. L. Phillips, J. Phys. Chem. A **104**, (2000).
[34] X. Zheng, W. M. Kwok, and D. L. Phillips, J. Phys. Chem. A (submitted).
[35] X. Zheng and D. L. Phillips, Chem. Phys. Lett. **316**, 524 (2000).
[36] M. Kawasaki, S. J. Lee, and R. Bersohn, J. Chem. Phys. **63**, 809 (1975).
[37] G. Schmitt and F. J. Comes, J. Photochem. **14**, 107 (1980).
[38] P. M. Kroger, P. C. Demou, and S. J. Riley, J. Chem. Phys. **65**, 1823 (1976).
[39] S. R. Cain, R. Hoffman, and R. Grant, J. Phys. Chem. **85**, 4046 (1981).

[40] B. J. Schwartz, J. C. King, J. Z. Zhang, and C. B. Harris, Chem. Phys. Lett. **203**, 503 (1993).
[41] K. Saitow, Y. Naitoh, K. Tominaga, and Y. Yoshihara, Chem. Phys. Lett. **262**, 621 (1996).
[42] A. N. Tarnovsky, J.-L. Alvarez, A. P. Yartsev, V. Sündstrom, and E. Åkesson, Chem. Phys. Lett. **312**, 121 (1999).
[43] J. Zhang and D. G. Imre, J. Chem. Phys. **89**, 309 (1988).
[44] J. Zhang, E. J. Heller, D. Huber, D. G. Imre, and D. Tannor, J. Chem. Phys. **89**, 3602 (1988).
[45] W. M. Kwok and D. L. Phillips, Chem. Phys. Lett. **235**, 260 (1995).
[46] W. M. Kwok and D. L. Phillips, J. Chem. Phys. **104**, 2529 (1996).
[47] F. Duschek, M. Schmitt, P. Vogt, A. Materny, and W. Kiefer, J. Raman Spectrosc. **28**, 445 (1997).
[48] M. Braun, A. Materny, M. Schmitt, W. Kiefer, and V. Engel, Chem. Phys. Lett. **284**, 39 (1998).